

Shape Memory Alloy Wire Actuators for Soft, Wearable Haptic Devices

George Chernyshov

Keio University Graduate
School of Media Design
Yokohama, Japan
chernyshov@kmd.keio.ac.jp

Feier Cao

Keio University Graduate
School of Media Design
Yokohama, Japan
feier@kmd.keio.ac.jp

Benjamin Tag

Keio University Graduate
School of Media Design
Yokohama, Japan
tagbenja@kmd.keio.ac.jp

Gemma Liu

Keio University Graduate
School of Media Design
Yokohama, Japan
gemmaliu@kmd.keio.ac.jp

Cedric Caremel

Keio University Graduate
School of Media Design
Yokohama, Japan
cedric@keio.jp

Kai Kunze

Keio University Graduate
School of Media Design
Yokohama, Japan
kai@kmd.keio.ac.jp

ABSTRACT

This paper presents a new approach to implement wearable haptic devices using Shape Memory Alloy (SMA) wires. The proposed concept allows building silent, soft, flexible and lightweight wearable devices, capable of producing the sense of pressure on the skin without any bulky mechanical actuators. We explore possible design considerations and applications for such devices, present user studies proving the feasibility of delivering meaningful information and use nonlinear autoregressive neural networks to compensate for SMA inherent drawbacks, such as delayed onset, enabling us to characterize and predict the physical behavior of the device.

ACM Classification Keywords

H.5.2 User Interfaces: Haptic I/O; H.5.m.Information Interfaces and Presentation (e.g. HCI)Miscellaneous

Author Keywords

Soft Robotics; Haptics; Wearable Devices; Shape Memory Alloys.

INTRODUCTION

The sense of touch is one of the oldest and most important senses that life on earth has developed. While primitive life forms such as nematodes have developed complex neural circuitry for touch perception [2], even the building blocks of complex life already show the ability to sense touch, e.g. eukaryote cells [10]. The human perception of touch relies on a more complicated somatosensory system [15]. Cutaneous senses are traditionally divided into four distinct modalities:

Permission to make digital or hard copies of all or part of this work for personal or classroom use is granted without fee provided that copies are not made or distributed for profit or commercial advantage and that copies bear this notice and the full citation on the first page. Copyrights for components of this work owned by others than the author(s) must be honored. Abstracting with credit is permitted. To copy otherwise, or republish, to post on servers or to redistribute to lists, requires prior specific permission and/or a fee. Request permissions from permissions@acm.org.

ISWC '18, October 8–12, 2018, Singapore, Singapore

© 2018 Copyright held by the owner/author(s). Publication rights licensed to ACM.
ISBN 978-1-4503-5967-2/18/10...\$15.00

DOI: [10.1145/3267242.3267257](https://doi.org/10.1145/3267242.3267257)



Figure 1. The prototype of a whole-finger haptic device with 3 SMA wire rings

tactile (pressure, vibration, etc), thermal (temperature), pruritic (itch), and pain [15, 14]. The tactile sensing modality can be further distinguished based on the cutaneous receptors responsible for sensing different stimuli. Whereas lamellar corpuscles are, together with their ability to sense pressure, especially sensitive to vibrations [26], the sense of pressure is mostly relying on the Merkel cells [13]. Both sensory stimuli are considered to follow the same neural pathways to the somatosensory cortex, they are complementary to each other rather than being two different sensing modalities.

In this paper, we present an alternative approach to traditional haptic interfaces that are mainly based on vibration and require the use of servomotors, solenoids or vibration motors. By utilizing Shape Memory Alloy (SMA) wires, we developed lightweight, soft, flexible, silent haptic actuators. The material is flexible, has a small diameter, is silent and ca-

pable of producing sufficient force for the device actuation. These properties open various interesting application cases for SMAs as actuators in soft haptic devices. Especially where the placement of hard mechanical actuators would sacrifice the wearability, user comfort, or design and appearance, SMA wires can be easily integrated and allow for an unobtrusive design, e.g. in wearables of various forms or smart garments. We demonstrate the viability of our approach by presenting and evaluating different SMA device designs in different use cases, discuss the advantages and disadvantages of our approach and the possible application scenarios.

Furthermore, we present user studies that demonstrate the possibility to deliver different kinds of information to the user using pressure based haptic sensations.

The main contributions of our work are threefold.

- We present and evaluate a novel approach to wearable haptic devices using SMA wires for giving pressure based haptic feedback. We implement several wearable prototypes and present insights in using the material.
- We compare our setup with traditional feedback methods.
- We propose a neural network model characterizing and predicting the behavior of the device, compensating for complicated thermo-physical properties of the prototypes.

RELATED WORKS

Soft Robotics

The field of traditional robot mechanics is mostly based on rigid skeletons, typically made of metal, mechanical joint bearings, and actuator. This often results in heavy setups that are only suitable for stable environments [12]. Apart from the previous traditional and rigid machine setting, new kinds of soft machines have been evolving from the research domains of rapid prototyping and proprioception. Soft robots offer a new approach to get rid of limitations well known to traditional robotics. Soft robotics utilizes their lifelike non-linear responses to actuation for motions and tasks in a relatively simple way [8]. Within this field of soft hardware, more specifically SMAs present with extremely reduced size, weight, and complexity compared to traditional machines [21]. Especially, because of SMAs extraordinary power-to-weight ratio and ease of construction, they are a suitable alternative for small robots [11]. For example, Fearing *et al.* [7] proposed a novel hexapedal walking millirobot using SMA. Their work is designed to achieve an alternating tripod gait with consideration of size and power constraints. Hino and Maeno created a miniature robot finger using SMA as the actuator [6]. Due to SMA wires' nonlinear features similar to human muscles, its structure is capable of imitating the musculoskeletal system of humans [11]. This adds to the compatibility with the human body, due to SMA's compact, lightweight, dexterous and powerful features.

Suhonen *et al.* [25] presented an early prototype, a wrist-type wearable using SMA to provide squeeze feedback in interpersonal communication. In their work, they linked the squeeze feedback to an emotional feeling of grip of a hand or a hug and concluded that compared to the other two vibrotactile and

thermal feedback, squeezes were regarded as the most pleasant type of haptic feedback. However, they only talked about the wrist-type wearable. Another work called HapticClench created by Gupta *et al.* [4] is a wrist-type wearable using SMA, which set the baseline study for both wrist-type and ring-type SMA. Using six different types of wires including SMA, they did a JND study and detected the thresholds of ring-type SMA, which is 0.25kg(95%CI[0.18,0.32]). This was helpful in our work.

Finger Augmentation Devices

In the realm of Human-Computer-Interfaces, haptic technology has gained great popularity because of its characteristics to bring additional feedback modalities to the field. For instance, as the research Virtual Reality (VR) and Augmented Reality (AR) develops and new application domains are explored, haptic feedback simulation is used more frequently to support more intuitive and immersive experience [23].

Finger augmentation devices became a major topic in the field due to the fact that fingers and fingertips show a high concentration of nerve cells and nerve endings enabling the recognition of even very subtle tactile stimuli [1]. Various actuators in finger augmentation devices and the primary and the most widespread being experimented was vibration [24]. Vibration is widely used to give haptic feedback [23], however, motors and coils are usually larger in size than SMA wire, and the vibration has tendencies to be irritating rather than expressive [22].

In comparison, non-vibratory feedback mainly comes in the form of compression and shear force. Non-vibratory devices promise to be less obtrusive than traditional vibration, because they can be designed using different types of actuators, such as electromagnetic, piezoelectric, and electrostatic actuators [23].

For example, Feng *et al.* [3] presented a wearable fingertip haptic display utilizing speakers to generate air pressure that inflates and deflates airbags. Pressure haptic feedback was also studied by Je *et al.* [9], who uses a solenoid in the form of a poking ring on the finger as an eyes-free human-computer-interface. The finger-wrap gives a direct pinching pressure on the finger. A different work by Minamizawa *et al.* [16] uses servomotors to generate vertical shearing force to create a weight sensation in VR environments that enable the simulation of gravity. Although the airbags are comparatively small on the finger, the speakers for pumping air are still large in size. A hand exoskeleton designed by Polygerinos *et al.* [19] uses soft actuators to augment hand rehabilitation, however, the setup is rather bulky.

PROOF OF CONCEPT

Design

In this section, we describe possible designs for different implementations. Considering the sensitivity of the palmar glabrous skin and the unique properties of the proposed approach we decided to concentrate on hand-worn devices only. They are in the form of a ring.

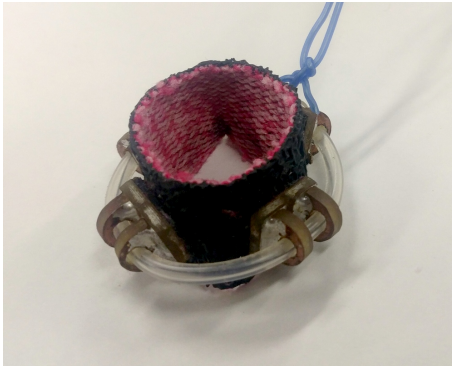


Figure 2. SMA wire ring with FR-4 supports and rubber coated fabric substrate.

Our approach relies on SMA wires (Biometal® Fiber BMF-150, D=150 microns, Toki corp.) for the device actuation. SMA's properties enable us to make our devices soft, lightweight, silent and flexible. BioMetal Fiber (BMF) is an anisotropically structured wire made of Nitinol (nickel-titanium alloy), which characteristically shrinks when heated. Additionally, its electrical properties allow resistive heating by simply applying an electric current to it. Using this property of the wire we built several prototypes discussed below, implementing our approach.

SMA Wire Ring

The evaluated devices are made of rings of SMA wire encapsulated into a silicone tube. The tube is attached to an elastic substrate using FR-4 or 3D-printed supports (See Fig. 2, 1). Since there is no insulation on the SMA wire by default, a silicone tube is meant to prevent the device from short-circuits and protect the users in case if the wire overheats as a result of a device malfunction or over-current. The haptic feedback is provided in form of pressure that results from SMA wire ring's contraction and expansion. Contraction and expansion of the wire can be controlled by varying the electric current using PWM or voltage regulation.

Haptic Glove

Using multiple rings placed on a glove, we made a haptic device capable of providing more complex feedback. For this prototype, we used one ring per each phalanx of the finger. Due to the small size of each ring, we could have placed more than three rings per finger, but for the sake of simplicity chose to use only three. Using this setup, we managed to present users with more complex feedback patterns and show the possibility of presenting numbers from 1 to 100 range.

Implementation

According to the manufacturer, one meter of BMF-150 wire produces a force of 144 gf when a current of 340 mA is applied. This significantly simplifies the control circuitry required to actuate the presented prototypes, reducing it to a single MOSFET or any other component that can act as a power switch. Even at 340 mA BMF-150 was perfectly capable of actuating

the presented devices and provide haptic sensations. However, most of the setups used currents higher than 340 mA to provide sharper feedback and faster contraction times.

Every device presented is actuated in a similar fashion. Devices are controlled by a STM32 NUCLEO-F446RE board and IRLML6344 power MOSFETs controlling current flowing through the BMF wire. MOSFETs are controlled with a 10 KHz PWM signal from F446RE. IRLML6344 is capable of handling up to 4A@10V currents, which is sufficient for multiple parallel SMA rings. It presents with an R(D-S) ranging from 29 to 37 mOhm, resulting in minimized voltage drops and heat emission. Moreover, it comes in a SMD SOT-23 package (approx. 2×3×1 mm including the pins), which makes it small enough to be incorporated in clothing or wearable devices.

Both of the implementations, the two rings, are capable of providing senses that traditionally require bulky mechanical actuators. Using SMA wire for actuation allowed us to make the devices soft, flexible, silent, small and lightweight. These characteristics are vital for the design of unobtrusive wearable devices. The capability of providing non-vibrational haptic feedback using the sense of pressure can open many new possible application scenarios, such as exploring the sense of affective touch or enabling more realistic haptic sensations for virtual environments.

USER STUDIES

In the following, we are going to explain the two user studies we ran in order to evaluate our prototypes.

Users were presented with a scenario where they had to recognize the haptic feedback and map it to data related to the hypothetical situation they were in. This adds complexity to the task, but makes the study more realistic and gives a good perspective on real-world application scenarios of the prototypes.

Study 1 - Applications

We conducted a series of studies, where we tested the possibility of providing information to the users using the glove prototype with three SMA rings on the index finger of the right hand, one ring per finger phalanx. Further on, the rings will be referred to by the name of the phalanx: proximal, intermedial, and distal.

In total eight users (Female: 4, Male: 4, Age: 19-27, AVG: 23.75, SD: 2.44) participated in two different application scenarios. In each scenario, we presented the users with a piece of information 10 times and asked users what information did they perceive. Users were wearing our device during the whole testing session. Two out of eight participants had smaller palm size and were not able to perceive some of the nuances. Since the ring size is not adjustable these participants were wearing an extra glove under the prototype, acting as an additional layer of substrate transferring the force to the participant's finger.

Bank Account Balance

In order to investigate the discriminability of different haptic patterns, we conducted a test were we presented users with

information regarding a hypothetical credit allowance. In total we expressed four possible conditions (100%, 66%, 33%, 0%) through different haptic patterns. For instance, one strong, long contraction (1500ms) on the proximal and intermedial phalanges, would be equal to 66% available from the credit allowance; a weak yet repetitive (three times), short (125 ms), contraction, on all the phalanges, suggested instead that the account was empty. We briefed the users on the device setup and the scale we were using. Then the participants were given a credit card, as soon as the card was touched, a pulse signal was sent, contracting the rings; then the practitioner was asking what is the card balance. The test resulted in an 81% accuracy for identifying the right credit balance, summarized in Fig. 3-A.

Timing Reminder

The second setting aimed at testing how haptic feedback presentation on different phalanges could be distinguished. For this purpose, we designed a "Timing Reminder" test. Each ring on the finger represented a train station on a train line. For the sake of this test the station closest to home was considered the destination and represented by the distal phalanx ring; the neighboring station, on the intermedial phalanx; the furthest station, on the proximal phalanx. Then the users were asked to imagine a scenario, where they are on a train bound home, and that they will be given haptic feedback representing the next station on their way. Then they were presented with a haptic sensation corresponding to one of the stations and asked what is the next stop. Users were able to determine the station correctly in 97.5% cases (see Fig. 3-B).

Progress Bar

For the last session, we were aiming at emulating a progress bar. It is worth noting that we used only three rings on the index finger to represent values ranging from 1% to 100%. We modulated the value using the timing of contraction and release on each phalanx. The sequence consists of 1000 ms in total. For lower percentages, the sequence was stopped at the time corresponding to the percentage. E.g. at 53% percent progress the sequence was interrupted at 530ms. Participants had a short training session, where they were showed how 100%, 75%, 50%, 25% and 15% would feel like. The sequence representing 100% was the following: 0ms - proximal contraction, 250 ms - intermedial contraction, 500 ms - proximal release and distal contraction, 750 ms - intermedial release, 1000 ms - distal release. After that, they were asked to estimate the progress of 10 sequences of random length. The results show that the average error is 9.61%, SD: 8.28, SE: 0.93 (see Fig. 4).

Study 2 - Reaction Time

In this study, we compared users' reaction time to the stimulus given through the SMA ring with the reaction times to either a visual stimulus (red LED, OSRAM LS M67K, 630nm, 14mcd, 120deg), an audible stimulus (2000 Hz sound from a piezo buzzer, manufacturer unknown), and vibro-haptic feedback (Nidec-Copal LD14-002 LRA driven with 5V power using A3909 Full bridge driver at 100 Hz frequency). Timing was controlled by an STM 32 NUCLEO-F446RE board with a

		Perceived			
		0%	33%	66%	100%
Actual	0%	14	1	0	0
	33%	0	15	0	2
	66%	0	1	16	5
	100%	0	4	2	20

		Perceived		
		0	1	2
Actual	0	23	0	0
	1	1	29	0
	2	1	0	26

Figure 3. Confusion matrices for the experiment "Bank Account Balance"(A) and "Timing Reminder"(B), 0 represents the "home station", 1 - a station away, 2 - two stations away

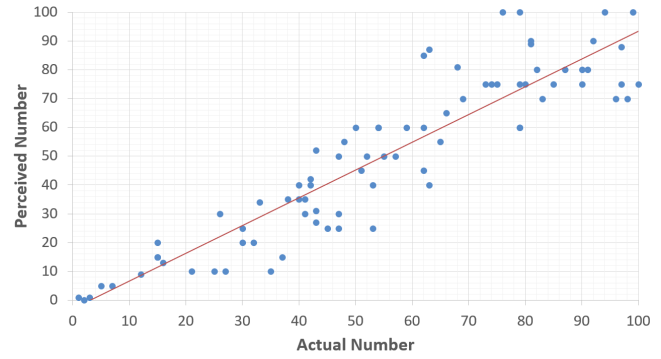


Figure 4. Progress Bar experiment confusion chart with trend line.

custom-made shield for feedback actuation. As the input device, we use a capacitive touchpad.

The LED was placed directly in front of the participants, the buzzer about 1 meter in front. Participants were wearing SMA ring on the index finger of their left hand. During the vibration reaction time test, the vibro-actuator was placed on the glabrous skin of the palmar side of the same phalanx of the finger as the SMA ring and fixated using Velcro tape. We used 3 Rings of different sizes to assure that the rings sit tightly on fingers of any size.

Experiment

The study was split into four sections of 20 stimulations per section. In each section, we used only one type of feedback. To eliminate the ordering effects we used a counterbalanced design. Participants were asked to touch the touchpad as quickly as they can after the stimulus onset using their right hand. The times between stimuli onsets were randomly selected from the 3000 - 10 000milliseconds range.

The measured average reaction times are as follows.

LRA 252.41ms ($SD = 55.65$)

LED 253.40ms ($SD = 47.50$)

AUDIO 232.19ms ($SD = 64.88$)

SMA 358.83ms ($SD = 78.95$)

Participants

16 users (female:7, male:9, age: 22-39 AVG:25.25, MED:25) participated in the experiment. The participants reported no

hearing or vision illnesses or disabilities nor any other health-related issues that could affect the study. Every participant had to give written consent to the study and was informed about the motivations, procedures, possible disadvantages, and benefits of the study.

Discussion

To investigate the causes of slower reaction time to SMA alloy wire rings contraction we filmed a series of contractions of the ring using a 960 fps camera (Sony RX100-V). Frame-by-frame visual analysis of the video showed that the ring contraction starts around 90-125ms after the current onset. As the current onset indicator, we used an LED. Furthermore, the expansion of the ring to its normal state was slow (3-4 seconds), which is probably caused by the silicone tube acting as a heat insulator. The estimated time and the contraction delay may vary depending on the thermal properties of the rings.

To provide crisp and distinguishable feedback the ring needs some resting time to cool down and come to its normal shape, otherwise, the perceived pressure is much weaker. The perceived sensation depends on many variables, such as the temperature of the wire, thermodynamics of the ring, ambient temperature, tension of the wire, etc. Most of these parameters have complicated non-linear effects on the physical behavior of the device. To overcome this problem we developed a model using neural networks characterizing the device and capable of predicting its behavior. Using a model that can predict the behavior of the device we can time the onset of the feedback as we please. This approach would allow synchronizing the onset of pressure-based haptic feedback with other devices or modalities that do not have an onset delay, e.g. visual or acoustic. This would enable us to design various cross-modal experiences using the sense of pressure. The modeling and results are discussed in the next section.

BEHAVIORAL MODEL AND PREDICTION

Providing crisp and distinguishable feedback using this approach requires to control the SMA actuators state precisely. However, due to the complexity of its behavior, it is hard to develop a good mathematical model of its behavior. However, as previously mentioned, one of our shape-memory alloy's main characteristic is that its behavior largely depends on exposure time and temperature, with persisting effects, such as how a short increase of the temperature may influence the displacement over a long period of time, even after the temperature has dropped. This has been described extensively in the literature and is otherwise known as the hysteresis behavior of SMA [20], a clear disadvantage that we also experience with Nitinol, the memory alloy we are using [18].

Several sophisticated models can be used to simulate the behavior of SMA, such as the Preisach model and the Jiles-Atherton model, both used for ferromagnetism; however, the recent advances in neural networks allow us to simulate non-linear systems with a minimal set of parameters [17]. This approach has been introduced by Wang *et al.* [5]. In our current setup, the difficulty is that the resting time needed after each contraction of the ring is hardly predictable with conventional methods. This resting parameter is critical in our

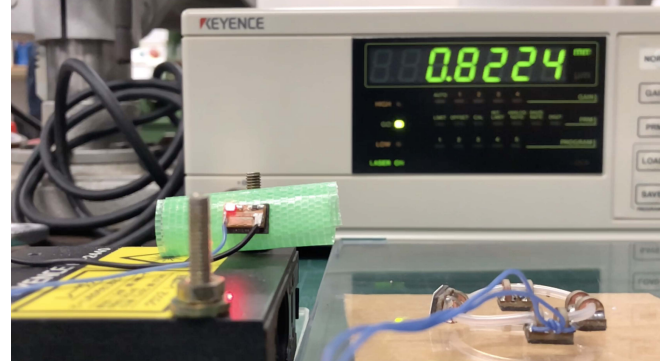


Figure 5. Picture of the test setup: a high accuracy laser displacement meter acquires a peak displacement of 0.8224 mm during contraction. The red LED indicates that the current is applied to the SMA, and was used for time synchronization.

testing sessions: understanding the hysteresis of the SMA can help us triggering adequately timed haptic feedback. Indeed, if the contraction peak is reached instantly after a current is applied to the SMA it takes more time for the ring to retrieve its original resting shape. The SMA cannot be quickly elongated unless it is forced-cooled, which would drastically complicate the design of our wearable device. Therefore, the state of the system is highly dependent on variables such as the room temperature and the devices' history. Although the room temperature can be easily controlled, the previous states of the system do not exhibit linearity, which makes prediction a difficult challenge. Therefore, anticipating the future states of the system is of crucial importance for a fully-controllable device.

Testing Setup

First, we designed a setup consisting of a high-speed/high accuracy laser displacement meter (Keyence LC-2400 with LC-2440 measuring head) measuring the contraction displacement relative to the sensor head, in a horizontal plane. As the silicone tube, containing the SMA wire, goes through four FR-4 supports (exerting pressure on the finger), a reflector was placed on one of them. This support was placed in front of the laser and the sensor was calibrated based on its reflectance. The three other supports were fixed on the horizontal plane so that each contraction would move the reflector only farther away from the sensor. The frictions to the horizontal plane, a slick plastic plate, were negligible at this scale, as the reflective marker could move freely without any significant difference compared to a test done in mid-air. The whole experiment was recorded at 240 fps. First, a constant current of 850mA, at 5V was applied to the SMA for 1s. The ring instantly contracted and we measured the displacement in mm, in the range 0.8004-0.881 (minimum-maximum). We repeated this procedure multiple times to evaluate the resting duration of the SMA ring, i.e. when the displacement measured by the sensor drops to near 0 (Fig. 5). It is worth noting the peak displacements by contraction are remarkably invariable over successive trials. However, the resting time is what is problematic here: after each short contraction, it takes more time for the alloy to

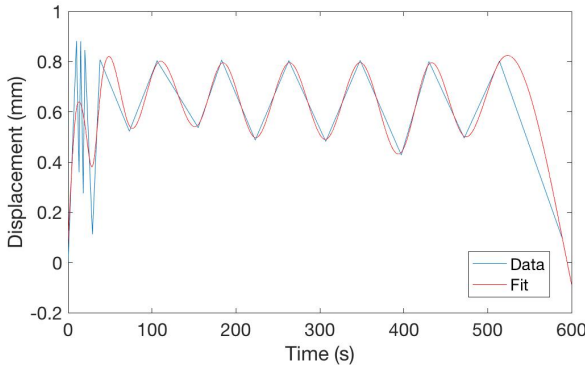


Figure 6. The simple fit, a spline interpolation between peak values, try to capture the nonlinear resting behavior of the SMA but does not properly describe all the characteristics of the alloy, especially the early stage (left values on the graph).

recover its original shape, which we assessed here over 10 successive trials, with 9 resting intervals (Fig. 7).

Behavioral Modeling

The data we collected in order to build a model consist in a time series that was acquired following the protocol described in the previous section and depicted in Fig. 5: we monitored the displacement dynamics of the ring by noting its magnitude and the associated time reference. Every time we triggered a contraction, the time it took for the ring to recover its original shape is not the same as previously noted. The resulting data, as shown in blue in Fig. 6, is as expected very noisy and therefore very difficult to model. Here, we want to use the right method to correctly assess the behavior of our SMA-actuated ring. Usually, smoothing methods are used to fit noisy data. We decided to test a conventional 'smoothing spline' model, using the MATLAB Curve Fitting toolbox: when calling the fit function, it returns a vector of values defined by the spline interpolation of x (time) and y (displacement). However, as shown in red in Fig. 6, only the values collected after about 1 min are properly fitted by this model; the displacement dynamic between 0 and 1 min is not well-captured. Indeed, the degree of the polynomial of the spline is high, with a relatively high Root Mean Square Error (RMSE) of 0.3391. A value closer to 0 would indicate that the fit is better for prediction. Likewise, the R-Squared error being weak at 0.6845, it performs better than a horizontal line, but the proportion of variance in the dataset is not fully captured by the fit.

Prediction using Neural Network

By stark contrast, we applied a Nonlinear Autoregressive Neural Network (NARX) to the model and it largely outperformed the simple fit, making it useful for prediction. The RMSE was evaluated at 0.0851 (1 order of magnitude smaller compared to the previous results with simple fit) and the R-squared error was 0.832, a clear indicator that the predictive model is robust.

Plotting the results of the NARX model compared to the original data (Fig. 8), we see how the early trials are now fully captured by the model. Besides, the main advantage of this

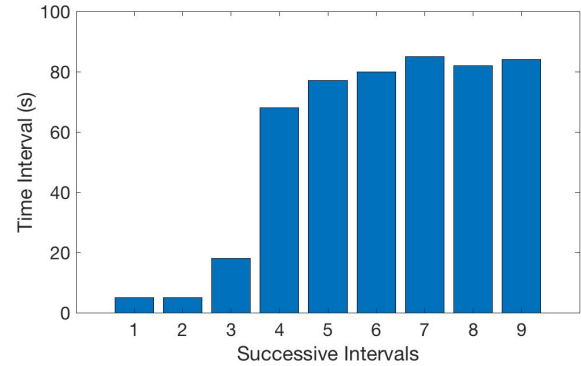


Figure 7. Resting time after displacement: it takes more time for the SMA to recover after successive contractions.

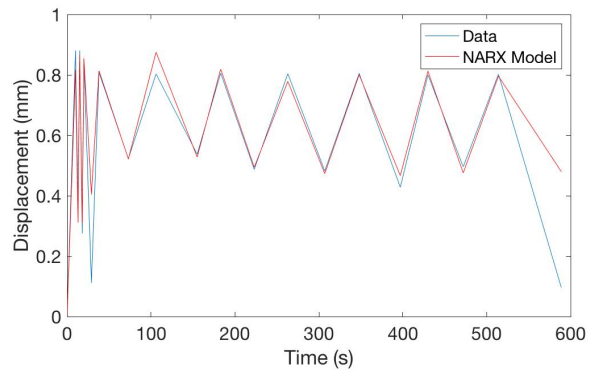


Figure 8. The Neural Network models and predicts the correct values much more accurately than the simple fit.

model architecture is that we could implement a predictive function. Unlike Wang *et al.* [5], we didn't use the Levenberg-Marquardt algorithm for the gradient descent but the Fletcher-Reeves conjugate method, giving fast results. Also, we only needed $n=8$ in our hidden layers (8 neurons) which we found was the optimal configuration for a better generalization across the repeat of the trained network. We divided the data into three subsets: the training set (60%), the validation set (20%) and the test set (20%), using the 'dividerand' function in MATLAB, with its 'divideMode' property set as 'time' for dynamic network. The results are shown in Fig. 10. The neural network computes the weights and biases of its network based on the training set. As the training advances, the error on this set will typically decrease. Meanwhile, a second set is used for validation: when the network starts to overfit the data, the error on the validation set, instead, increases: the training is stopped (Fig. 9).

The third set, the testing set, is never used while training to ensure that we can objectively evaluate the performance of the trained model over a new set of data. We run the neural network multiple times until we get a satisfying model that generalizes well, without over-fitting. The linear regression value R between outputs and targets on the training, validation and test sets is $R=0.97$ (1 is ideal) for the test set, see Fig. 10.

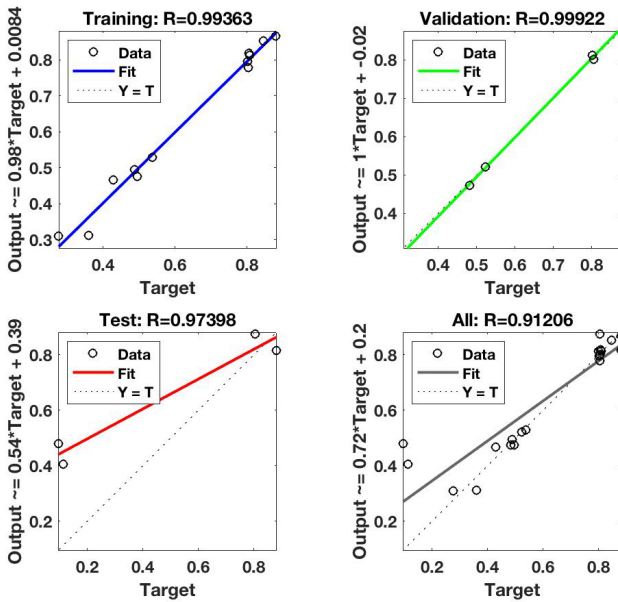


Figure 10. The four sub-plots represent the training, validation, and testing data. The colored lines represent the best fit linear regression line between outputs and targets, with the value R defining the relationship between outputs and targets.

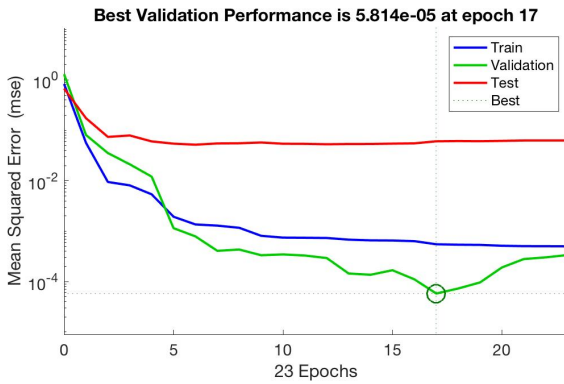


Figure 9. Best validation performance (mse) of the training, validation and test set. The error on the validation set increases after epoch 17, signaling the network starts to overfit the data. The weights and biases are selected at this minimum for the training set. The error on the test set, although higher, also decreases, showing similitudes with the training set trend.

There is no over-fitting as both the training error and the testing error converge to a small mean square error (Fig. 9) and, more importantly, the predicted values were consistently in the range previously mentioned, around 0.8–0.9 mm displacement, meaning that the features of the system were correctly assessed by the model: short burst of contraction with a displacement at a maximum peak below 1 and relax state duration based on nonlinear dependencies relative to the history of the system.

CONCLUSION AND FUTURE WORK

In this paper, we propose an interesting approach to wearable haptic device actuation enabling us to provide the sense of

pressure, in a soft, flexible and lightweight form, unlike traditional mechanical actuators. We demonstrate the feasibility of using SMA wires and pressure for haptic feedback in a series of studies, where the participants were able to recognize the information they were presented with. We also present our characterization of the device using neural networks, capable of predicting the device’s behavior. Our model enables simple timing and modeling of the crucial thermal and physical properties of the device, and provides feedback, rendering complicated calculations unnecessary.

The proposed design solutions minimize the drawbacks, inherent to SMA wires, e.g. we propose the usage of silicone tubes to serve as heat insulators. Moreover, we utilize a NARX model to successfully predict the device’s onset delay and increase of necessary resting period after consecutive contractions. In future works, we plan to explore the subjective perception of the pressure haptic sense provided by the prototypes. Using various senses and modalities opens the way for many interesting research questions, especially in the domains of cross-modal feedback and subjective perception of haptic interfaces.

ACKNOWLEDGMENTS

This work is supported by JST CREST Grant Number JP-MJCR16E1.

REFERENCES

- Mohamed Benali-Khoudja, Moustapha Hafez, Jean-Marc Alexandre, and Abderrahmane Kheddar. 2004. Tactile interfaces: a state-of-the-art survey. In *Int. Symposium on Robotics*, Vol. 31. Citeseer, 23–26.
- M. Chalfie, JE. Sulston, JG. White, E. Southgate, JN. Thomson, and S. Brenner. 1985. The neural circuit for touch sensitivity in *Caenorhabditis elegans*. *Journal of Neuroscience* 5, 4 (1985), 956–964. DOI: <http://dx.doi.org/10.1523/JNEUROSCI.05-04-00956.1985>
- Yuan-Ling Feng, Charith Lasantha Fernando, Jan Rod, and Kouta Minamizawa. 2017. Submerged haptics: a 3-DOF fingertip haptic display using miniature 3D printed airbags. In *ACM SIGGRAPH 2017 Emerging Technologies*. ACM, 22.
- Aakar Gupta, Antony Albert Raj Irudayaraj, and Ravin Balakrishnan. 2017. HapticClench: Investigating Squeeze Sensations using Memory Alloys. In *Proceedings of the 30th Annual ACM Symposium on User Interface Software and Technology*. ACM, 109–117.
- Gangbing Song Han Wang. 2014. Innovative NARX recurrent neural network model for ultra-thin shape memory alloy wire. *Elsevier, Neurocomputing* 134 (2014).
- Toshiyuki Hino and Takashi Maeno. 2004. Development of a miniature robot finger with a variable stiffness mechanism using shape memory alloy. In *International Symposium on Robotics and Automation, Querétaro, México, Aug. 25–27*.

7. Aaron M Hoover, Erik Steltz, and Ronald S Fearing. 2008. RoACH: An autonomous 2.4 g crawling hexapod robot. In *Intelligent Robots and Systems, 2008. IROS 2008. IEEE/RSJ International Conference on*. IEEE, 26–33.
8. Filip Ilievski, Aaron D Mazzeo, Robert F Shepherd, Xin Chen, and George M Whitesides. 2011. Soft robotics for chemists. *Angewandte Chemie* 123, 8 (2011), 1930–1935.
9. Seungwoo Je, Minkyong Lee, Yoonji Kim, Liwei Chan, Xing-Dong Yang, and Andrea Bianchi. 2018. PokeRing: Notifications by Poking Around the Finger. In *Proceedings of the 2018 CHI Conference on Human Factors in Computing Systems (CHI '18)*. ACM, New York, NY, USA, Article 542, 10 pages. DOI: <http://dx.doi.org/10.1145/3173574.3174116>
10. H. S. Jennings. 1899. Studies on Reactions to Stimuli in Unicellular Organisms. III Reactions to Localized Stimuli in Spirostomum and Stentor. *The American Naturalist* 33, 389 (1899), 373–389.
11. Mohammad Mahdi Kheirikhah, Samaneh Rabiee, and Mohammad Ehsan Edalat. 2010. A review of shape memory alloy actuators in robotics. In *Robot Soccer World Cup*. Springer, 206–217.
12. Cecilia Laschi and Matteo Cianchetti. 2014. Soft robotics: new perspectives for robot bodyware and control. *Frontiers in Bioengineering and Biotechnology* 2 (2014).
13. Srdjan Maksimovic, Masashi Nakatani, Yoshichika Baba, Aislyn M. Nelson, Kara L. Marshall, Scott A. Wellnitz, Pervez Firoz Firozi, Seung-Hyun Woo, Sanjeev Sumant Ranade, Ardem Patapoutian, and Ellen A. Lumpkin. 2014. Epidermal Merkel Cells are Mechanosensory Cells that Tune Mammalian Touch Receptors. In *Nature*.
14. Francis McGlone and David Reilly. 2010. The cutaneous sensory system. *Neuroscience and Biobehavioral Reviews* 34, 2 (2010), 148 – 159. DOI: <http://dx.doi.org/10.1016/j.neubiorev.2009.08.004> Touch, Temperature, Pain/Itch and Pleasure.
15. Francis McGlone, Johan Wessberg, and HÅkan Olausson. 2014. Discriminative and Affective Touch: Sensing and Feeling. *Neuron* 82, 4 (2014), 737 – 755. DOI: <http://dx.doi.org/10.1016/j.neuron.2014.05.001>
16. Kouta Minamizawa, Souichiro Fukamachi, Hiroyuki Kajimoto, Naoki Kawakami, and Susumu Tachi. 2007. Gravity grabber: wearable haptic display to present virtual mass sensation. In *ACM SIGGRAPH 2007 emerging technologies*. ACM, 8.
17. Ho Pham Huy Anh Nguyen Ngoc Son. 2015. Adaptive displacement online control of shape memory alloys actuator based on neural networks and hybrid differential evolution algorithm. *Elsevier, Neurocomputing* 166 (2015).
18. Fabio Díaz Palacios, Maritza Irahola Zalles, Jhon Ordoñez Ingali, Diego Rojas Arancibia, and Gabriel Rojas Silva. 2015. *Mechanical features analysis of the Nitinol alloy under microgravity conditions*. Technical Report.
19. Panagiotis Polygerinos, Zheng Wang, Kevin C.Galloway, Robert J. Wood, and Conor J.Walsh. 2015. Soft robotic glove for combined assistance and at-home rehabilitation. In *Robotics and Autonomous Systems*, Vol. 73. Elsevier, 135–143.
20. A. Pruski and H. Kihl. 1993. Shape memory alloy hysteresis. In *Sensors and Actuators A: Physical*. Elsevier.
21. Daniela Rus and Michael T. Tolley. 2015. Design, fabrication and control of soft robots. *Nature* 521 (2015), 467–475.
22. Saar Shai. 2011. Finger-worn device and interaction methods and communication methods. (Sept. 1 2011). US Patent App. 13/049,925.
23. Roy Shilkrot, Jochen Huber, Jürgen Steinle, Suranga Nanayakkara, and Pattie Maes. 2015. Digital digits: A comprehensive survey of finger augmentation devices. *ACM Computing Surveys (CSUR)* 48, 2 (2015), 30.
24. Robert J Stone. 2001. Haptic feedback: a brief history from telepresence to virtual reality. In *Haptic Human-Computer Interaction*. Springer, 1–16.
25. Katja Suhonen, Kaisa Väänänen-Vainio-Mattila, and Kalle Mäkelä. 2012. User experiences and expectations of vibrotactile, thermal and squeeze feedback in interpersonal communication. In *Proceedings of the 26th Annual BCS Interaction Specialist Group Conference on People and Computers*. British Computer Society, 205–214.
26. J. Zelená. 1994. *Nerves and Mechanoreceptors: The Role of Innervation in the Development and Maintenance of Mammalian Mechanoreceptors*. Springer Netherlands.